Carpathian Journal of Earth and Environmental Sciences, February 2022, Vol. 17, No. 1, p. 5 – 20; DOI:10.26471/cjees/2022/017/196

INSIGHTS INTO THE ORIGIN OF SHALLOW MARINE DOLOSTONES, LONGWANGMIAO FORMATION (LOWER CAMBRIAN), NORTHEAST SICHUAN BASIN, CHINA: PETROGRAPHIC AND GEOCHEMICAL CONSTRAINTS

Jian WANG[1,2,3]*, Lu ZHOU[1,2], Baozhen ZHANG[4] & Chonglong GAO[5]

*[1]State Key Laboratory of Oil and Gas Reservoir and Exploration, Southwest Petroleum University, Chengdu 610500, China, *Corresponding author: wangjian_0990@126.com*

[2]School of Geosciences and Technology, Southwest Petroleum University, Chengdu 610500, China

[3]Research Institute of Experiment and Detection, PetroChina Xinjiang Oilfield Company, Karamay 834000, China

[4]Fengcheng Oil field Operation District, Xinjiang Oilfield Company Petrochina, Karamay, Xinjiang 834000, China

[5]Institute of Unconventional Oil & Gas, Northeast Petroleum University, Daqing 163318, China

Abstract: For a better understanding of the origin of Early Cambrian dolomites in the Sichuan Basin, which serve as valuable oil and gas reservoirs, we present and interpret complex multiparameter petrographic and geochemical analyses of dolomites in the Cambrian Longwangmiao Formation at the Yangsiqiao section. Our data show that these dolomites mainly occur in the middle and upper parts of the Longwangmiao Formation, and we identify two types of dolomites: micrite and fine-medium crystalline dolomites. The micritic dolomites, occasionally coupled with quartz and mica minerals, show dirty crystal surfaces, nonautogenous crystal shapes, and dark cathodoluminescence and mainly occur in pure micrite and granular dolostones, which retain the original sedimentary texture. Contrarily the fine-medium crystalline dolomites, mainly developed in crystalline and grain dolostones and generally coupled with residual calcites and altered sedimentary textures, have a dark heart-bright boundary texture under a polarized microscope and occasional zonal texture under cathode luminescence. Furthermore, the micritic dolomites have CaO and MgO contents approximately similar to those of the ideal stoichiometric dolomite, relatively high Sr concentration, Σ rare-earth element (REE) +Y concentrations, and $\delta^{13}C$ and $\delta^{18}O$ values located in the corresponding range of dolomite deposited from Early Cambrian marine water. However, light-REE enrichment (LREE), heavy-REE (HREE) depletion patterns, and high Al_2O_3 and SiO_2 contents distinguish these micritic dolomites from typical marine carbonate deposits. Notably, the fine-medium crystalline dolomites have higher CaO content and lower MgO, Al_2O_3 and SiO_2 contents, lower Sr and higher Fe and Mn concentrations than those of micritic dolomites. The ΣREE+Y concentrations and REE patterns of these fine-medium crystalline dolomites belong to the typical marine carbonate deposits. These features indicate considerable differences in origins between micrite and fine-medium crystalline dolomites. The micritic dolomites show a significant genetic response to the precipitation of seawater in shallow marine with the injection of terrestrial water during the syngenetic period, while the fine-medium crystalline dolomites have a typical response to the secondary metasomatism products of original calcites at the shallow burial stage.

Keywords: petrological features, geochemical features, origin of dolomite, oil and gas reservoirs, Early Cambrian

1. INTRODUCTION

1.1. Previous Research Status

The Cambrian Longwangmiao Formation gas reservoir in the Sichuan basin is the largest discovered Cambrian gas reservoir in the world (Du et al., 2014; Zou et al., 2014; Li et al., 2017). Previous studies have shown that the reservoir of the Cambrian Longwangmiao Formation in the Sichuan Basin, mainly composed of dolostones, possesses a large thickness, pervasive distribution, and favorable reservoir performance (Ren et al., 2015; Wang et al., 2019a). However, pores, caves, and fractures in the dolostone stratum dominantly constitute the reservoir space and have a complex configuration relationship, leading to the extremely strong heterogeneity of the reservoir (Wang et al., 2019b). Furthermore, these studies have mainly focused on the qualitative and quantitative description of petrological characteristics in addition to the spatial and physical characteristics of the Longwangmiao Formation reservoir (Ren et al., 2015; Yang et al., 2015; Zhou et al., 2015; Li et al., 2017; Sun et al., 2018; Wang et al., 2019b). Therefore, because of scarce research on dolomites' origin and water-rock reactions, the genetic mechanism of the favorable reservoir in the Longwangmiao Formation is unknown.

1.2. Significance of This Study

The genesis of dolomites is an important topic considered in the studies of the favorable reservoir in the Longwangmiao Formation, because dolomitization influences the reservoir as an essential water-rock reaction. Researchers have mostly adopted petrological and mineralogical characteristic analyses of dolostone in the Longwangmiao Formation to infer the dolomites' origin, but multiple papers reported isotopic and elemental data during last decade. However, these papers did not identify and illustrate the differences and interrelations between petrological and geochemical parameters, providing scant evidence and deficient inferences. Therefore, studies on the dolomites' origin and the dolomitization process show a lack of precise depiction and unified cognition, restraining the genetic mechanism study of the favorable reservoir in the Longwangmiao Formation.

In this paper, we precisely depict the petrological and geochemical characteristics of the Longwangmiao Formation dolostones using frequent and sequential sampling at the Yangsiqiao section in the northeast Sichuan Basin. We systematically present and interpret complex petrological parameters (mineral composition, crystal structure, and the order degree of dolomites) and geochemical parameters (major, trace, and rare-earth element concentrations, relative ratios, and stable isotopic compositions) of the dolomites. Furthermore, we ascertain the dolomites' petrogenetic origin as well as the source of dolomitization fluids and preliminarily reconstruct the dolomitization environment and process. This paper integrates petrological, mineralogical, elemental and isotopic evidence and proves that the formation of the Cambrian Longwangmiao Formation dolomites has been a continuous process from depositional to burial environments stimulated by different dynamic mechanisms of the multiple phases of fluids. Furthermore, the Cambrian Longwangmiao Formation dolomites mainly have two forms based on the precipitation of seawater, with the injection of terrestrial water and the replacement of previous calcites through the water-rock reaction. Therefore, this paper is significant for studying the effect of dolomitization on the reservoir's performance and predicting a favorable reservoir.

2. GEOLOGICAL SETTING

2.1. Location of the Studied Section

The Yangsiqiao section is situated near the cities of Chengkou and Zhenping in Sichuan Province, belonging to the transitional belt between the Sichuan Basin and the Qinling orogenic belt with a specified location at the south part of the Chengkou-Zhenping nappe (Fig. 1a). In the Chengkou-Zhenping area, outcrops contain multiple sets of strata from the Ediacaran to the Quaternary with the exception of the Devonian, Carboniferous, and Cretaceous. The Lower-Middle Cambrian strata comprise the following conformable lithostratigraphic units in ascending stratigraphic order: Qiongzhusi, Canglangpu, Longwangmiao and Gaotai; the Longwangmiao Formation exhibits conformable contacts with both the overlying Gaotai Formation and the underlying Canglangpu Formation.

2.2. Lithology and Paleogeography of the Cambrian Longwangmiao Formation

With a thickness of 55-290-m, the Cambrian Longwangmiao Formation in the studied area mainly comprises dolostone and a small amount of limestone as well as evaporate and dolomitic siltstone. During the depositional period of the Longwangmiao Formation, the studied area developed carbonate platforms characterized by multiple granular shoals and could be subdivided into restricted and open platforms (Ren et al., 2016; Sun et al., 2018; Zhang et al., 2019). The Yangsiqiao section is located in the granular shoal of the open platform (Fig. 1b). Furthermore, the Longwangmiao Formation at the Yangsiqiao section, approximately 290m thick, shows an upward lithological transition from limestone to dolostone, and 25 layers can be identified according to lithological classification, containing seven layers of dolostone with a cumulative thickness of 86.9m (Fig. 1c). Furthermore, significant lithology shifts occur at the boundaries among the underlying strata, the Longwangmiao Formation, and the overlying strata, respectively (Fig. 1c).

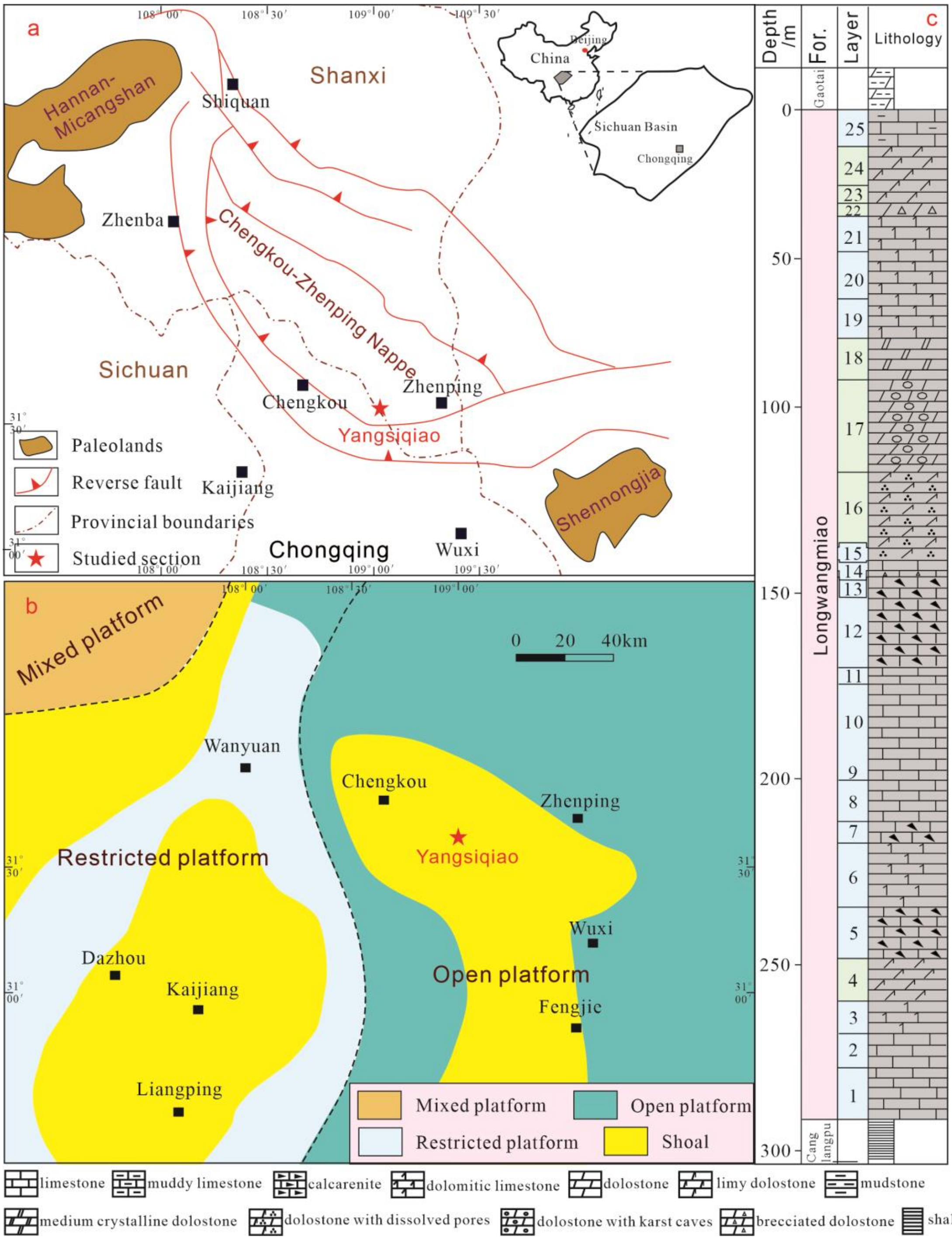

Figure 1. Location, structure, lithology, and lithofacies paleogeography of the Longwangmiao Formation in the northeast Sichuan Basin (modified from Zhang et al., 2019).

3. SAMPLING AND ANALYTICAL TECHNIQUES

3.1. Sampling and Petrological Analysis

In this study, we obtained dolostone samples from the Longwangmiao Formation continuously at the Yangsiqiao section in 2-m intervals; 43 dolostone samples were finally collected. Moreover, all samples were obtained from fresh outcrops to avoid obvious weathering and calcite veins. According to the comprehensive filed study, the dolostone samples predominantly comprise crystalline dolostone, oolitic dolostone, dolarenite, and argillaceous dolostone. To accurately identify the petrological characteristics (composition, textures, diagenetic phase, and relationships of grains, matrix, cement, and fractures), all thin sections were stained with alizarin red and examined using an Olympus Microscope BH-2 light optical microscope. Cathodoluminescence microscopy of polished thin sections was performed using a CL8200-MK5 cathodoluminescence system with a beam voltage of 15kV, beam current of 400μA, and a vacuum degree at 0.003mbar.

3.2. X-ray Diffraction, Elemental, and Stable Isotopic Composition Analyses

To avoid veins filled with silicalite or calcite and diagenetic alteration areas as well as eliminate the influence of carbonate heterogeneity, we obtained the samples by drilling at the most homogeneous part of the freshly cut surfaces from hand specimens using a 1-mm drill bit. The samples were finely powdered successively using iron and agate mortars into 200μm. Finally, the obtained powder was divided into three parts for X-ray diffraction (XRD), elemental, and stable isotopic composition analyses. XRD was conducted using a Bruker D2 PHASER X-ray diffractometer at the state key laboratory of oil and gas resources and exploration, China University of Petroleum (Beijing). According to the industry standards of quantitative analysis of whole-rock XRD (SY/T 5163-2010), XRD was conducted under operating conditions of 30kV, 10mA, a scanning rate of 2° 2θ/min, and with CuKα radiation and whole-rock random-powder patterns recorded from 4.5° to 50° (2θ). Only 31 dolostone samples possessed relatively high purity with dolomite contents ≥75% and Mg/Ca ratios ≥ 0.125 according to XRD analysis. Additional studies for the other samples using elemental and stable isotopic composition analyses would be worthless because they contained massive impurities.

The major elements analyses, conducted at Beijing Research Institute of Uranium Geology using the Philips PW2404 X-ray fluorescence spectrometer, were according to the China National Standard method for determining 16 major and minor element contents of the silicate rocks (GB/T 14506.28-2010). Trace and REE analyses, conducted using element XR inductively coupled plasma (ICP) mass spectrometer (MS) (ICP-MS), were according to the China National Standard method for determination of 44 elements in silicate rocks (GB/T14506.30-2010).

The carbon and oxygen isotope analyses were conducted at the State Key Laboratory of Petroleum Resource and Prospecting, China University of Petroleum (Beijing). The analyses were conducted using a MAT 253 gas mass spectrometer equipped with a Kiel IV carbonate device. To extract CO_2 and avoid dissolving detrital minerals, anhydrous phosphoric acid was reacted with dolostone powders in vacuum at 25°C for 24h. The results, based on replicate analyses of GBW 04405, are given using conventional $\delta^{13}C$ and $\delta^{18}O$ notations following the Vienna Pee Dee Belemnite (VPDB) standard with the analytical error at ± 0.1‰.

4. PETROLOGICAL ANALYSES

The fieldwork, thin sections, cathode luminescence, and XRD analyses show that the dolostones of the Longwangmiao Formation at the Yangsiqiao section are mainly composed of micritic and fine-medium crystalline dolomites, showing significant differences in petrographic characteristics in terms of crystal sizes, textures, and diagenetic phase.

4.1. Micritic Dolomites

Micritic dolomites occur in pure micritic and granular dolostones, whereas several samples also contain small amounts of quartz and mica (Table 1). They appear in the form of a matrix or are composed of carbonate grains (Fig. 2a-e). Further, micritic dolomites generally <50μm— show noneuhedral crystals with dirty surfaces and exhibit nonluminescence or dark luminescence (Fig. 2c). Moreover, micritic dolomites exhibit two types of occurrences: 1) widespread on one side of the stylolite, serving as a lithological change interface, because the other side of the stylolite comprises pure micritic calcites (Fig. 2d); and 2) clustered together as particles (Fig. 2e).

4.2. Fine-Medium Crystalline Dolomites

Fine-medium crystalline dolomites dominantly comprise crystalline, granular and limy dolostones (Table 1), occurring as particles or residual particles (Fig. 2f-i). The fine-medium crystalline dolomites range in size from 50 to 150μm and commonly exhibit euhedral or-subhedral crystals. Moreover, the fine-medium crystalline dolomites generally possess a foggy center-clear rim texture (Fig. 2f-g), showing clear oscillatory zoning and bright-red light in cathodoluminescence images (Fig. 2h). The fine-medium crystalline dolomites usually occur in the form of mottled assemblages in residual granular dolostones and even several particles only remnant on visible grain boundaries or stripes (Fig. 2i), or in the form of scattered distribution in the matrix (Fig. 2f) or closely surround the rims of grains.

5. GEOCHEMISTRY

5.1. Major Elements

The major element data of the Longwangmiao Formation dolostones at the Yangsiqiao section are given in Table 2. Dolostones comprising micritic dolomites have CaO content ranging from 14.97% to 43.27% with an average value of 29.69%, and MgO content ranging from 10.28% to 23.85% with an average value of 17.25%. However, their CaO and MgO contents do not correlate (Fig. 3a), and Mg/Ca ratios range between 0.37 and 1.49 with an average value of 0.81 (Table 2). Furthermore, dolostones comprising fine-medium crystalline dolomites show CaO content ranging from 31.31% to 47.66% with an average value of 37.55% and MgO content ranging from 7.14% to 20.66% with an average value of 12.13%. No correlation exits between CaO and MgO contents but their Mg/Ca ratios are low, ranging from 0.21 to 0.89 with an average value of 0.45 (Table 2). Thus, the micritic dolomites discussed herein contain low CaO and MgO contents and Mg/Ca ratios compared with ideal stoichiometric dolomites (30.0%, 21.70% and a unit, respectively). Fine-medium crystalline dolomites have high CaO content and obviously low MgO content as well as Mg/Ca ratios (Fig. 3a). Previous studies have confirmed that most dolomite components have been just slightly altered during dolomitization, and partial geochemical nature has been well preserved during the recrystallization (Machel, 1997; Kaczmarek & Sibley, 2011; Ren et al., 2019a). Therefore, the higher MgO content and Mg/Ca ratios of micritic dolomites compared with the corresponding values of fine-medium crystalline dolomites indicate that the dolomitization fluids of micritic dolomites should obtain higher Mg/Ca ratios and their dolomitization shows a faster rate accordingly.

Table 1 Mineral compositions of the dolostones in the Longwangmiao Formation, northeast Sichuan Basin

Sample	Lithology	Dolomite	Calcite	Quartz (%)	Feldspar	Clay
Y1	Micritic dolostones	70.6	4.2	14.0	0	9.8
Y2	Micritic dolostones	57.6	42.4	0	0	0
Y3	Micritic dolostones	60.9	35.4	3.7	0	0
Y4	Micritic dolostones	61.6	33.8	4.6	0	0
Y5	Micritic dolostones	63.9	0	12.5	0	21
Y6	Micritic dolostones	64.1	0	7.8	0	3.3
Y7	Micritic dolostones	64.1	35.6	0.3	0	0
Y8	Micritic dolostones	68.2	0	23.9	0	3.3
Y9	Micritic dolostones	75.3	1.3	12.5	0	5.4
Y10	Micritic dolostones	69.7	3.8	22.2	0	0
Y11	Argillaceous dolostones	54.1	1.2	13.6	3.3	27.8
Y12	Micritic dolostones	52.5	18.5	20	0	7.2
Y13	Micritic dolostones	56.9	42.4	0.7	0	0
Y14	Micritic dolostones	71.2	1.2	11.1	0	15.6
Y15	Crystalline dolostones	96.6	0	3.4	0	0
Y16	Micritic dolostones	97.9	2.1	0	0	0
Y17	Micritic dolostones	68.9	24.8	2.2	0	0
Y18	Micritic dolostones	80.8	0.5	5.7	0	0
Y19	Micritic dolostones	79.5	16.2	2.1	0.7	1.5
Y20	Crystalline limy dolostones	75.6	14.7	5.5	0	0
Y21	Crystalline limy dolostones	97.9	0	0.9	1.3	0
Y22	Micritic dolostones	81.8	0	12.8	0	4.4
Y23	Micritic dolostones	83.7	0	7.2	0	8.1
Y24	Dolarenite	85.6	2.6	10.1	0	1.7
Y25	Micritic dolostones	88.0	1.7	5.1	0	0
Y26	Micritic dolostones	94.3	1.5	4.1	0	0
Y27	Micritic dolostones	94.6	1.5	1.8	0	0
Y28	Micritic dolostones	95.1	4.2	0	0	0
Y29	Micritic dolostones	99.6	0	0.1	0	0.4
Y30	Micritic dolostones	97.7	0	0.9	1.3	0
Y31	Oolitic dolostones	99.6	0	0.2	0	0.2

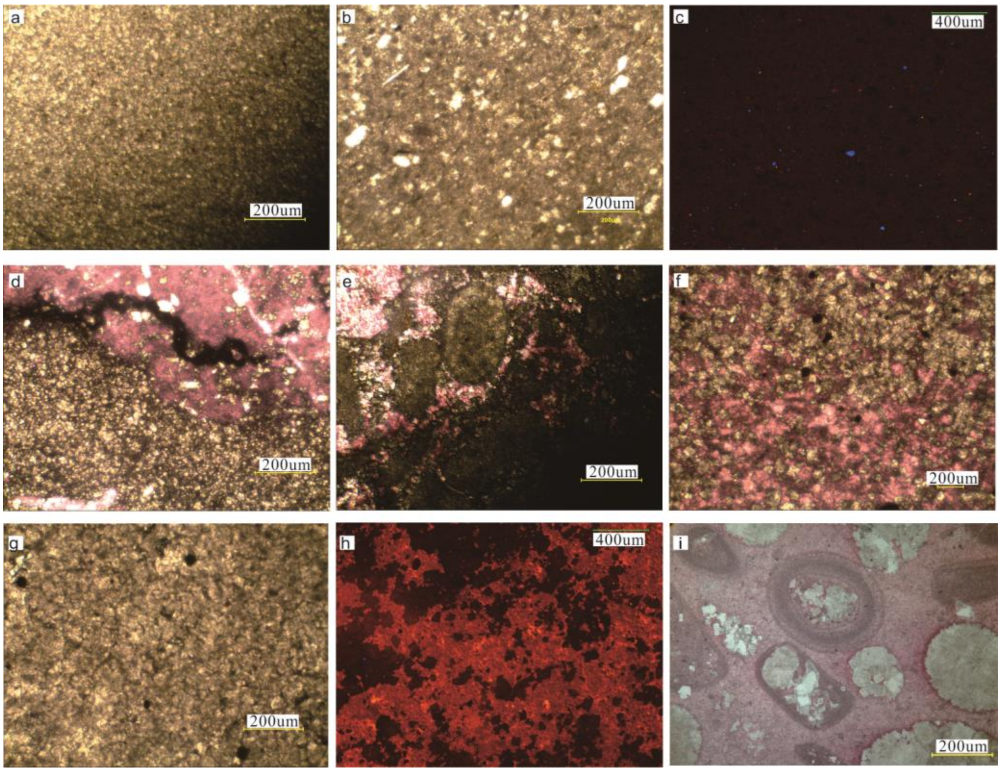

Figure 2. Petrological, microscopic, and cathode luminescence characteristics of dolomites in the Longwangmiao Formation, northeast Sichuan Basin. (a) Sample Y8, pure micritic dolomites, plane-polarized light. (b) Sample Y11, massive micritic dolomites with quartz and micas, plane -polarized light. (c) Cathode luminescence of Sample Y11, dolomites with dark-brown light and quartz with blue light. (d) Sample 13, stylolite shown as the boundary line between calcites and dolomites on each side, alizarin red stain for calcites, and plane -polarized light. (e) Sample 24, grains composed of micritic dolomites and matrix with micrite calcites, alizarin red stain for calcites, and plane -polarized light (f) Sample 16, the randomly distributed fine-crystalline dolomites and calcites, alizarin red stain for calcites, and plane -polarized light. (g) Sample 21, fine-to-medium crystalline dolomites, plane -polarized light. (h) Cathode luminescence of Sample Y21, dolomites with red light. (i) Sample 31, fine-crystalline dolomites in residual oolitic grains, alizarin red stain for calcites, and plane-polarized light.

In addition, dolostones comprising micritic dolomites have high Al_2O_3 and SiO_2 contents with values ranging from 0.18% to 7.64% and 0.04% to 2.23%, respectively. Dolostones comprising fine-medium crystalline dolomites have low Al_2O_3 and SiO_2 contents with values less than 0.46% and 1.07%, respectively (Table 2). These differences in Al_2O_3 and SiO_2 contents indicate that the dolomitization process of micritic dolomites might have been influenced by relatively massive terrestrial influxes coinciding with their petrological characteristics occasionally concurrent with quartz and mica. However, the influence of terrestrial influxes on the dolomitization of fine-medium crystalline dolomites would be insignificant.

5.2. Trace Elements

According to the trace element analysis (Table 1), the Sr concentrations in dolostones composed of micritic dolomites vary from 55.80 ppm to 213.70 ppm, Mn concentrations vary from 94.40 ppm to 429.04 ppm (sample Y3 had an abnormally high value and was removed from the statistical analysis). Fe concentrations range from 2110.57 ppm to 26121.48 ppm, where their Mn/Sr ratios vary from 0.90 to 7.12 (Table 2). Nevertheless, the dolostones composed of fine-medium crystalline dolomites contain low Sr concentrations and significantly high Fe and Mn concentrations. Mn/Sr ratios are also higher compared with the corresponding values of the dolostones composed of micritic dolomites, since their Sr concentrations range from 33.82 ppm to 108.70 ppm, Fe concentrations vary from 1687.07 ppm to 54912.55 ppm, Mn concentrations vary from 144.22 ppm to 1243.55 ppm, and Mn/Sr ratio range from 2.42 to 23.85.

Previous studies illustrated that Sr depletion as well as Fe and Mn enrichment frequently occur during the dolomitization process. The Fe and Mn concentrations exhibit significant enrichment covariation with the increase in the burial depth (Anderson, 1989; Allan & Wiggins, 1993; Ren et al.,

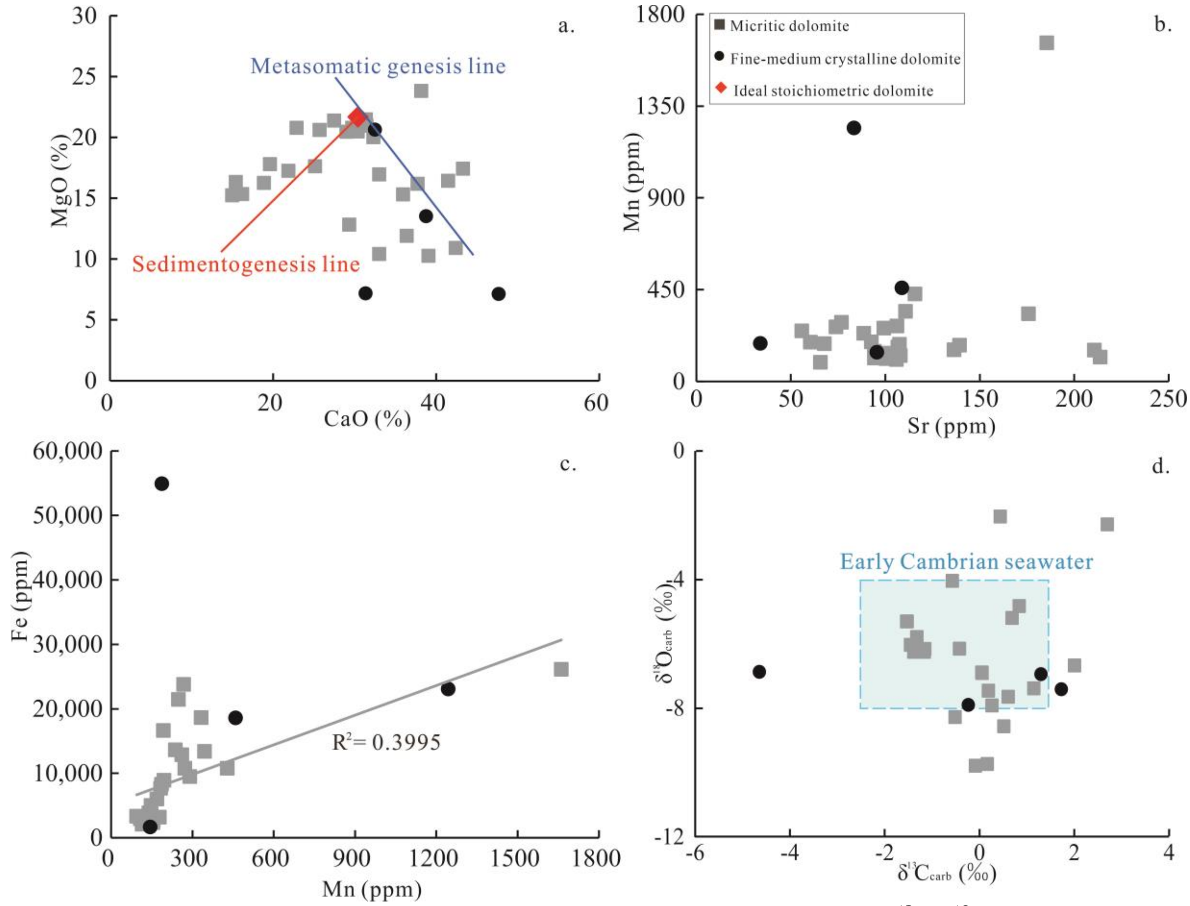

Figure 3. Cross plot of CaO-MgO (%) (a), Sr-Mn (ppm) (b), Mn-Fe (ppm) (c), and $\delta^{13}C$-$\delta^{18}O$ (‰) (d) of dolomites in the Longwangmiao Formation, northeast Sichuan Basin (the trends of the sedimentogenesis and metasomatism lines are from Ren et al., 2016 and the $\delta^{13}C$-$\delta^{18}O$ scope of Early Cambrian seawater is from Veizer et al., 1999).

2019b). Therefore, we infer that the differences in Sr, Fe, and Mn concentrations between these two types of dolostones could be attributed to the increasing postdepositional and burial diagenesis, illustrating that the dolomitization of micritic dolomites would occur before that of the fine-medium crystalline dolomites. Furthermore, these indicate that the dolomitization fluids of the fine-medium crystalline dolomites are rich in Fe and Mn, which might have external sources contributing to the increased availability of these elements. Furthermore, both types of dolostones have no correlation between Sr and Mn concentrations (Fig 3b) as well as between Mn and Fe concentrations (Fig 3c). Therefore, Mn and Fe could have various sources or unsynchronized behaviour during the dolomitization process (Mriheel & Anketell, 2000; Zhao & Jones, 2012; Ren et al., 2019b).

5.3. Rare-Earth Elements

Marine carbonates contain low ΣREE+Y concentrations (from 1 ppm to 50 ppm), and their REE patterns exhibit typical LREE-depletion and HREE-enrichment patterns (Fallon et al., 2002; Bolhar et al., 2004; Johannesson et al., 2006; Zhao and Zheng, 2017; Ren et al., 2019b). The dolostones composed of micritic dolomites have ΣREE+Y concentrations ranging from 6.27 ppm to 58.80 ppm with an average of 24.50 ppm (Table 2) and distinct LREE-enrichment and HREE-depletion patterns (Fig. 4a). Their dolomitization fluid was presumably influenced by terrestrial influx, consistent with the petrological characteristics and Al_2O_3 and SiO_2 content analyses. Meanwhile, the ΣREE+Y concentrations of the dolostones composed of fine-medium crystalline dolomites vary from 7.15 ppm to 76.99 ppm with an average of 45.67 ppm, and their rare earth elements show LREE-depletion and HREE-enrichment patterns (Fig. 4b), correlating with the corresponding characteristics in marine carbonates.

Furthermore, the calculated Ce/Ce* values of micritic dolomites range from 0.67 to 1.12 with an average value of 0.90. The other type dolomites have Ce/Ce* values varying from 0.81 to 1.04, with an average value of 0.92. The majority of dolomites in the Longwangmiao Formation yield negative Ce anomalies with Ce/Ce* values less than 1.00, coinciding with the corresponding characteristics of carbonates formed in oxidized surface seawater.

Table 2. Major, trace and rare earth elemental concentrations and stable isotopic compositions of dolomites in the Longwangmiao Formation at the Yangsiqiao section, northeast Sichuan Basin

Micritic	CaO	MgO	Al_2O_3	SiO_2	Sr	Mn	Fe	Mn/Sr	Mg/Ca	$\delta^{13}C$	$\delta^{18}O$	T	REE	Eu/	Ce/
dolomites	(%)				(ppm)			-		VPDB/‰		/°C	$/10^{-6}$	Eu*	Ce*
Y1	33.00	10.42	1.95	0.61	213.70	120.43	3130.05	0.90	0.44	0.04	-6.88	21.90	19.00	0.76	0.85
Y2	33.00	16.97	0.80	0.57	210.70	154.15	2320.78	1.17	0.72	0.05	-6.90	21.99	24.52	0.36	0.82
Y3	38.16	23.85	2.01	0.65	185.40	1660.89	26121.48	14.33	0.87	0.83	-4.82	13.34	50.77	0.99	0.78
Y4	25.67	20.62	2.19	0.85	100.40	111.96	3140.83	1.78	1.12	-1.53	-5.30	15.27	21.97	1.12	0.88
Y5	27.45	21.39	2.14	0.62	105.90	108.26	2949.10	1.64	1.09	-1.54	-5.30	15.27	23.84	0.75	0.98
Y6	31.44	20.98	0.80	0.25	106.60	169.02	6007.54	2.54	0.93	-0.52	-8.27	28.13	21.99	1.44	0.94
Y7	31.34	21.51	0.76	0.24	98.86	139.14	3874.64	2.25	0.96	-0.52	-8.27	28.13	20.66	1.11	0.95
Y8	28.97	20.47	0.46	0.17	107.40	182.49	7673.82	2.72	0.99	-1.33	-5.78	17.24	16.06	1.20	1.06
Y9	25.11	17.64	2.23	0.59	94.19	147.84	5003.46	2.51	0.98	-1.33	-5.78	17.24	13.45	0.70	1.02
Y10	19.59	17.82	3.39	2.02	73.86	268.19	23780.68	5.81	1.27	-1.46	-6.03	18.28	46.16	0.87	0.83
Y11	14.97	15.24	6.11	2.23	55.80	248.17	21477.61	7.12	1.43	-0.58	-4.04	10.29	31.52	1.56	1.01
Y12	32.30	20.03	3.90	0.91	175.80	332.10	18660.18	3.02	0.87	0.18	-7.45	24.41	36.64	0.64	0.84
Y13	30.35	20.50	1.49	0.50	110.60	344.81	13413.40	4.99	0.95	0.16	-6.86	21.81	38.56	1.28	0.99
Y14	21.86	17.27	7.64	1.81	88.60	236.54	13657.49	4.27	1.11	-0.43	-6.14	18.74	32.27	0.85	0.89
Y16	15.40	16.35	5.22	2.21	60.24	192.65	16618.91	5.12	1.49	-1.17	-6.24	19.16	44.40	0.50	0.67
Y17	22.87	20.80	5.21	1.51	99.20	261.34	12855.15	4.22	1.27	-1.35	-6.13	18.70	29.47	1.13	0.91
Y18	16.20	15.34	4.33	2. 50	76.69	290.21	9481.01	6.05	1.33	-1.39	-6.24	19.16	25.31	8.36	0.83

Y19	18.84	16.28	4.49	1.76	92.56	194.81	8938.16	3.37	1.21	-1.16	-6.15	18.78	30.74	1.09	0.85
Y22	41.44	16.44	0.42	0.18	115.70	429.04	10790.01	5.93	0.56	-0.09	-6.94	22.16	58.80	1.46	0.96
Y23	36.36	11.92	1.43	0.51	108.00	127.28	2962.96	1.89	0.46	0.60	-7.64	25.26	7.74	1.04	1.04
Y24	37.71	16.20	0.18	0.04	94.75	133.29	2517.90	2.25	0.60	0.26	-7.91	26.48	10.47	0.01	0.87
Y25	39.03	10.28	1.41	0.33	136.30	155.62	2741.97	1.83	0.37	0.43	-2.04	2.89	9.38	0.01	0.73
Y26	43.27	17.44	0.82	0.17	65.66	94.40	3346.42	2.30	0.56	2.00	-6.67	20.99	11.90	0.31	1.12
Y27	42.37	10.94	0.42	0.16	139.20	177.79	3209.36	2.04	0.36	0.51	-8.56	29.48	8.42	1.25	0.68
Y28	29.33	12.84	2.36	0.81	106.10	272.43	10779.23	4.11	0.61	1.14	-7.38	24.09	9.20	0.02	0.97
Y29	29.70	20.79	0.75	0.22	94.26	114.58	2110.57	1.94	0.98	0.68	-5.19	14.82	11.90	1.16	0.96
Y30	35.93	15.33	0.79	0.15	67.68	185.96	8312.92	4.40	0.60	2.69	-2.28	3.75	6.27	2.35	0.97
Average	29.69	17.25	2.36	0.84	110.52	119.71	9106.50	3.50	0.81	-0.18	-6.19	19.18	24.50	0.92	0.90
Fine-medium	CaO	MgO	Al_2O_3	SiO_2	Sr	Mn	Fe	Mn/Sr	Mg/Ca	$\delta^{13}C$	$\delta^{18}O$	T	REE	Eu/	Ce/
crystalline	/%				$/10^{-6}$			mol/mol		VPDB/‰		/°C	$/10^{-6}$	Eu*	Ce*
Y15	31.31	7.19	0.46	1.07	108.70	458.92	18584.72	6.76	0.32	-4.65	-9.73	35.11	22.83	0.60	1.04
Y20	32.46	20.66	0.42	0.00	83.43	1243.55	23063.04	23.85	0.89	-0.24	-7.89	26.39	76.99	0.91	0.96
Y21	47.66	7.14	0.01	0.01	33.82	187.65	54912.55	8.88	0.21	1.29	-9.78	35.36	75.71	0.86	0.89
Y31	38.75	13.54	0.06	0.35	95.50	144.22	1687.07	2.42	0.49	1.72	-7.40	24.18	7.15	1.22	0.81
Average	37.55	12.13	0.24	0.36	80.36	508.59	24561.85	10.13	0.45	-0.47	-8.70	30.26	45.67	0.90	0.92

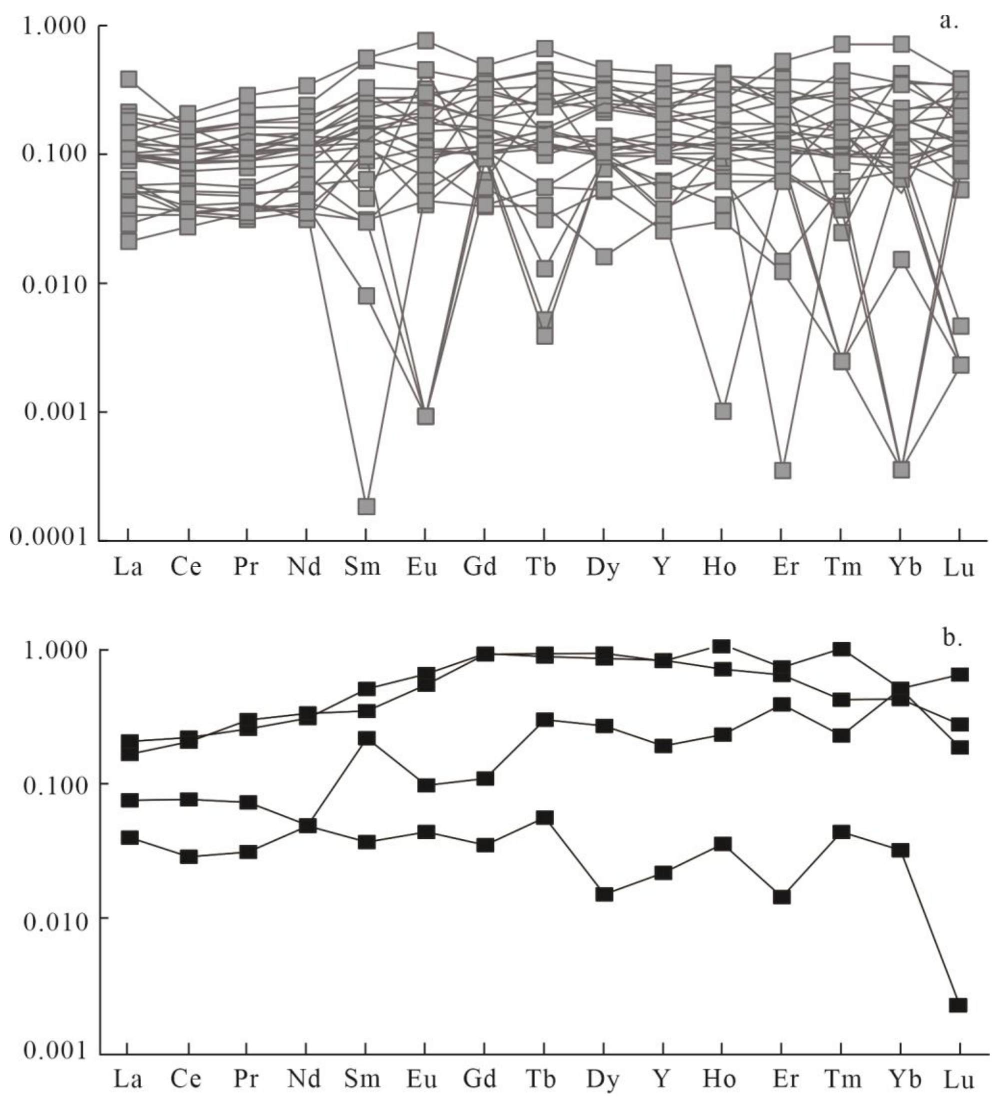

Figure 4. REE+Y patterns of micritic dolomites (a) and fine-medium crystalline dolomites (b) in the Longwangmiao Formation, northeast Sichuan Basin.

5.4. Carbon and Oxygen Isotope

The Early Cambrian seawater showed $\delta^{13}C$ values varying from -2.50‰ to 1.50‰ and $\delta^{18}O$ values from -8.00‰ to -4.00‰ (Veizer et al., 1999; Montańze et al., 2000; Jiang et al., 2016; Ren et al., 2019b). In the Longwangmiao Formation, dolostones composed of micritic dolomites have $\delta^{13}C$ values ranging from -1.54‰ to 2.69‰ with an average value of -0.18‰ and $\delta^{18}O$ values ranging from -9.73‰ to -2.04‰, with an average value of -6.40‰ (Table 2). The other type of dolostones feature relatively low $\delta^{13}C$ values from -4.67‰ to 1.72‰ with an average value of -0.47‰ and $\delta^{18}O$ values from -7.89‰ to -6.86‰ with an average value of -7.27‰. Therefore, the majority of dolostones in the Longwangmiao Formation yield $\delta^{13}C$ values in a similar range to Cambrain seawater (Fig. 3d). Moreover, calcite has a depleted $\delta^{18}O$ value at the range around 2.00‰ compared with the contemporaneous dolomite from the same solution at the same temperature because of the difference in the isotopic fractionation factor between these two carbonate minerals (Land, 1980; McKenzie, 1981; Vasconcelos et al., 2005). However, the dolostones of the Longwangmiao Formation have lower $\delta^{18}O$ values than the Early Cambrian seawater and the prodolomite deposited from the initial seawater.

The $\delta^{13}C_{carb}$ values are predominantly influenced by depositional fluid natures and buried organic materials other than temperature, postdepositional diagenesis, and burial depth (Banner & Hanson, 1990; Banner, 1995; Melanie, 2006), and they generally retain primary isotopic signatures during the diagenesis process. Whereas the $\delta^{18}O_{carb}$ values are more sensitive to penecontemporaneous or postdepositional diagenesis seen in the oxygen isotope exchange with meteoric/burial water. Therefore, in the absence of correlation between $\delta^{13}C$

and $\delta^{18}O$ values of dolostones in the Longwangmiao Formation (Fig. 3d), the dolomitic fluid of the Longwangmiao Formation might be derived from contemporaneous seawater. Thus, we infer that the $\delta^{18}O$ depletion could be attributed to external fluids (e.g., terrestrial influx) during the depositional stage or the compaction-derived fluids from seawater that might have been liberated at slightly higher temperatures with increasing burial depth.

In addition, $\delta^{18}O_{carb}$ values are widely used to reconstruct the temperature during carbonate precipitation (Vasconcelos et al., 2005) via equations based on $\delta^{18}O$ values of both the carbonate minerals and the solution from which they precipitate (Friedman & O'Neil, 1977).

$$1000 \ln \alpha_{\text{dolomite-water}} = 3.06 \times 10^{6}\, T^{-2} - 3.24$$

where: T= carbonate precipitation temperature, $\alpha_{\text{dolomite-water}}$ = oxygen isotope of dolomite depositional water.

We take the medium $\delta^{18}O$ value (-6‰) of Early Cambrian seawater as the optimized oxygen isotopic composition of the precipitation fluid and $\delta^{18}O_{dol}$ values of the Longwangmiao Formation dolostones (Table 2) in the equation to calculate the temperature during dolomite precipitation. Notwithstanding other factors, the calculated results show that the formation temperature of micritic dolomites ranges from 10.29℃ to 29.48℃ with an average value of 19.18℃. Fine-medium crystalline dolomites exhibit higher precipitation temperatures ranging from 21.81℃ to 35.36℃ with an average value of 30.26℃. Because the paleogeothermal gradient is approximately 27℃/km (Zhu et al., 2016), the difference in the formation depth between these two types of dolomites is approximately 410m. This conclusion reinforces the notion derived from former petrological and elemental analyses that the precipitation of micritic dolomites occurred earlier than the fine-medium crystalline dolomites.

6. DISCUSSION

6.1. Origin of the Micritic Dolomites

The primary textures of dolomites are considered a crucial evidence of their origin because the different crystal sizes and shapes of dolomites presumably reflect variable formation temperatures and distinguished dynamics of nucleation and growth (Sibley & Gregg, 1987; Zhang et al., 2014; Bao et al., 2019). Therefore, micritic dolomites and fine-medium crystalline dolomites in the Longwangmiao Formation tended to precipitate at different stages under distinct dynamic conditions. The micritic dolomites of the Longwangmiao Formation exhibit multifarious beddings on a macroscopic scale Moreover, original sedimentary texture, tiny crystals with the absence of secondary metasomatism in microscope together with dark cathodoluminescence images can also be identified. Because the prodolomite has a tiny micritic crystal and no obvious diagenetic alteration, the characteristics of micritic dolomites reveal that these dolomites acquired petrological signatures when precipitating during the syngenetic stage when the sediments were still unconsolidated. Furthermore, the micritic dolomites yield Mg/Ca ratios and CaO and MgO contents approximately corresponding to the values of ideal dolomite, such as Ce/Ce* anomalies similar to the typical marine carbonates, $\delta^{13}C$ values in the corresponding range of Early Cambrian seawater, and an average calculated precipitation temperature at 19.18℃. These geochemical features may indicate that these dolomites formed next to the sediment-water interface during the syngenetic stage, where the pore water mainly derived from the shallow seawater.

Previous studies have demonstrated that the Sichuan Basin was influenced by massive terrestrial influxes during the depositional period of the Longwangmiao Formation (Ren et al., 2019b), particularly during the early depositional period (Fig.5a-b). In addition, the high Al_2O_3 and SiO_2 contents, LREE-enrichment and HREE-depletion patterns, and the occurrence of quartz and mica in several samples (Fig. 2b) reveal that terrestrial influxes might be involved in the subsurface water of shallow marine. The dilution of seawater, increased temperature, and alkalinity of dolomitization fluid could help overcome the dynamic obstacles for the formation of dolomite (Mei, 2012). The northeast Sichuan Basin tended to be favorable for the development of the mixing water dolomitization during the Longwangmiao Stage.

Therefore, the integrated analyses of the geological background as well as petrological and geochemical characteristics demonstrate that the micritic dolomites of the Longwangmiao Formation were formed during the syngenetic period and their dolomitization fluid was a mixture of shallow surface seawater and terrestrial water (Fig. 5c). Moreover, the majority of the Longwangmiao Formation dolomites had already formed during the syngenetic period because micritic dolomites have the most widespread distribution in this formation.

6.2. Origin of Fine-Medium Crystalline Dolomites

Petrologic analysis shows that the fine-medium crystalline dolomites are characterized by large size, dirty crystal face, foggy center-clear rim texture, clear oscillatory zoning, and bright-red light in cathodoluminescence images. Furthermore, fine-medium crystalline dolomites in dolostone have distinct occurrences in microscopic features: 1) commonly scattered in a matrix accompanied by calcites, and several calcites only remaining as residuals because of the incomplete replacement of calcites by dolomite; 2) clustered together in the interior of residual particles, which are mainly composed of calcites and dolomites because of the incomplete replacement of calcites by dolomite. The complete replacement rarely occurs, leading to particles only remaining visible at grain boundaries. These petrological features suggest a metasomatic genesis, derived from water-rock reactions during the postdepositional stage as products of the replacement of calcites.

In addition, the geochemical features of fine-medium crystalline dolomites also indicate a metasomatic genesis. With high CaO content but low MgO content and Mg/Ca ratios comparable with the corresponding values of ideal dolomite, fine-medium crystalline dolomites tend to be derived from the incomplete dolomitization process concurrent with the insufficient replacement of Ca^{2+} by Mg^{2+}, reinforcing the inference derived from petrological features. Moreover, fine-medium crystalline dolomites showed an average precipitation temperature of 30.26℃, calculated using the $\delta^{18}O$ value, which is higher than that of micritic dolomites. Correspondingly, they showed an increase in the

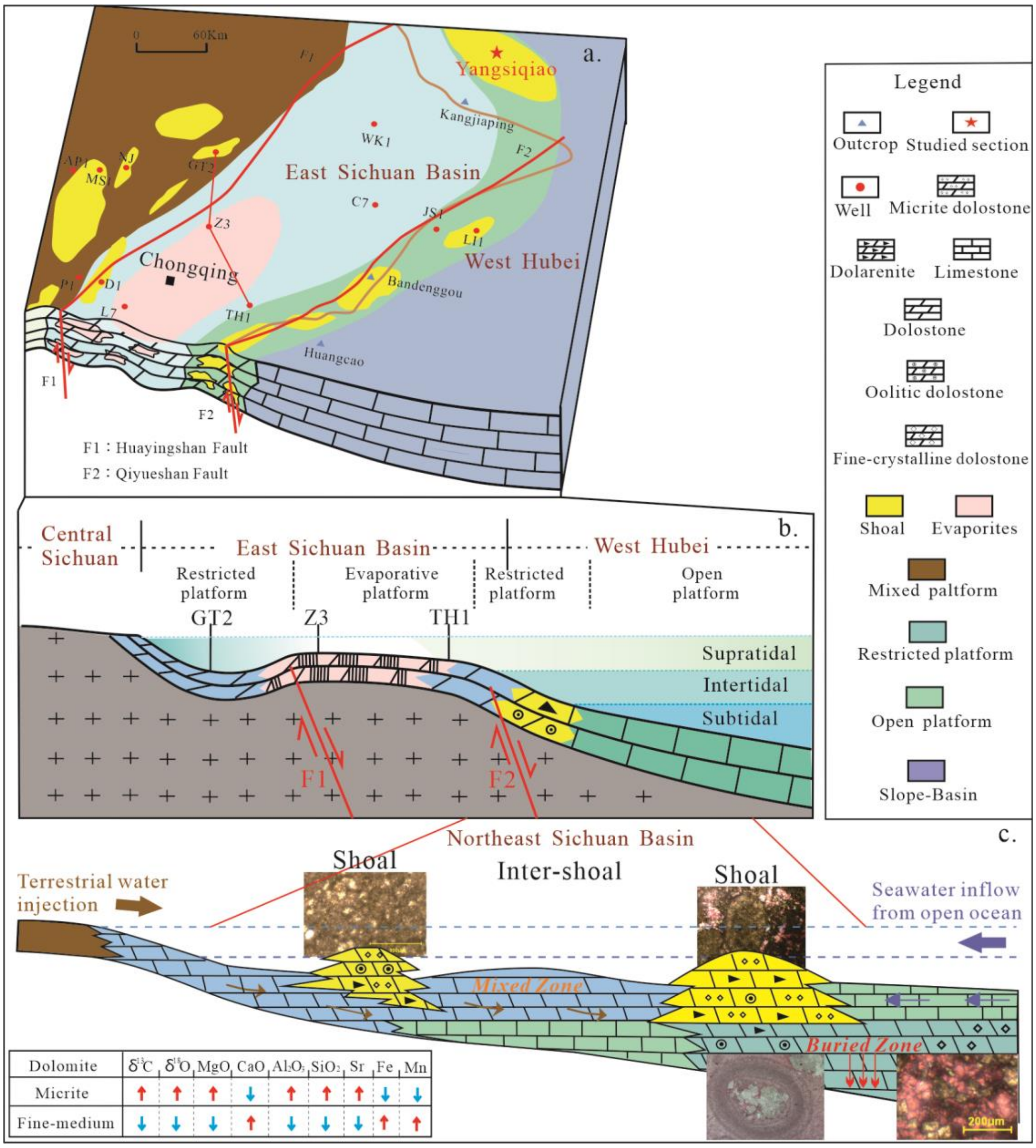

Figure 5. Sedimentary pattern ((a) and (b); modified after Ren et al., 2016) and the development model (c) of different types of dolomites in the Cambrian Longwangmiao Formation in the northeast Sichuan Basin.

formation depth with an average value of 410.37m according to the paleogeothermal gradient. Because micritic dolomites precipitated during the syngenetic period, fine-medium crystalline dolomites formed during the shallow burial stage, and the increasing temperature with the burial helped overcome the kinetic barrier of dolomite formation. Compared with micritic dolomites, fine-medium crystalline dolomites yielded low Sr concentrations and high Fe and Mn concentrations, indicating a later formation stage because Sr-depletion as well as Fe and Mn enrichment during the dolomitization process exhibit significant covariation with the increase in the formation depth. This is consistent with the interpretation derived from the calculated precipitation temperature using the $\delta^{18}O$ value and formation depth by the paleogeothermal gradient. The low Al_2O_3 and SiO_2 contents, typical LREE-depletion and HREE-enrichment patterns and the absence of quartz and mica indicate the metasomatism genesis of fine-medium crystalline dolomites with a dolomitization fluid having marine parentage.

Therefore, the integrated analyses of geological background as well as petrological and geochemical features demonstrate that the fine-medium crystalline dolomites of the Longwangmiao Formation products of secondary metasomatism other than an authigenic overgrowth of micritic dolomites were formed through the replacement of original calcites with a marine-parentage fluid during the shallow burial period (Fig. 5c). However, this replacement might be incomplete considering the widespread residual calcites and less development of fine-medium crystalline dolomites.

The significant differences in petrological and geochemical characteristics between micritic dolomites and fine-medium crystalline dolomites indicate that these two types of dolomites were subjected to different precipitation environments, formation fluids, and dynamic mechanisms.

7. CONCLUSIONS

The Longwangmiao Formation mainly contains widespread micritic dolomites and slight fine-medium crystal dolomites. Micritic dolomite mainly occur in pure micritic and granular dolostones and retain the original sedimentary structure. The micritic dolomites, generally less than 50μm, show nonlluminescence crystals with a dirty surface and exhibit mostly nonluminescence or dark luminescence, occasionally alongside quartz and mica. The fine-medium crystalline dolomites dominantly comprise crystalline, granular and limy dolostones. These crystalline dolomites with sizes ranging from 50 to 150μm exhibit euhedral or semi-euhedral crystals, foggy center-clear rim texture, clear oscillatory zoning, and bright-red light in cathodoluminescence images, commonly accompanied by calcites or residual calcites after replacement.

Significant differences exist in the geochemical characteristics between micritic dolomites and fine-medium crystalline dolomites in the Longwangmiao Formation. The micritic dolomites possess Mg/Ca ratios and CaO and MgO contents correlating with the corresponding values of ideal dolomite, relatively high Al_2O_3 and SiO_2 contents, $\delta^{13}C$ values located in the corresponding range of Early Cambrian seawater, relatively high Sr concentrations, ΣREE+Y concentrations, and Ce/Ce* anomalies similar to typical marine carbonates. However, their REE+Y patterns differ from those of marine carbonates with high LREE-enrichment and HREE-depletion. Compared with micritic dolomites, fine-medium crystalline dolomites show high CaO content, low MgO, Al_2O_3, and SiO_2 contents; slightly low $\delta^{13}C$ and $\delta^{18}O$ values; low Sr concentrations; high Fe and Mn concentrations; and low ΣREE+Y concentrations. However, their REE+Y patterns are similar to those of typical marine carbonates.

The significant differences in petrological and geochemical characteristics between micritic dolomites and fine-medium crystalline dolomites in the Longwangmiao formation indicate that these two types of dolomites were subjected to different precipitation environments, formation fluids, and dynamic mechanisms. Micritic dolomites exhibit significant genetic responses to the precipitation from the mixture of seawater in shallow marine with the injection of terrestrial water during the syngenetic period. Fine-medium crystal dolomites have a typical response to the metasomatism genesis, as the products of the reaction between original calcites and marine-parentage fluid during the shallow burial period, other than the merely authigenic overgrowth of micritic dolomites.

Acknowledgments

We are indebted to the Southwest Oil and Gas field Company, PetroChina Company Limited, China for providing data and software technology support.

REFERENCES

Allan, J.R., **& Wiggins, W.D.** 1993. *Dolomite reservoirs: geochemical techniques for evaluating origin and distribution*. Tulsa: AAPG Continuing Education Course Note Series, 36, 19-32.

Bao, Z.D., **Ji, H.C.**, **Liang, T.**, **Wei, M.Y.**, **Shi, Y.Q.**, **Li., Z.F.**, **Lu, K. & Xiang, P.F.** 2019. *Primary dolostones of the Meso-Neoproterozoic, cases on typical platforms in China*. Journal of Palaeogeography (Chinese Edition), 21, 869-884.

Banner, J.L. & Hanson, G.N. 1990. *Calculation of simultaneous isotopic and trace element variations during water-rock interaction with application to carbonate diagenesis*. Geochimica et Cosmochimica Acta, 54, 3123-3138.

Banner, J.L. 1995. *Application of the trace element and isotope geochemistry of strontium to studies of carbonate diagenesis*. Sedimentology, 42, 805-824.

Bolhar, R., **Kamber, B.S.**, **Moorbath, S.**, **Christopher, M.F. & Martin, J.W.** 2004. *Characterisation of early Archaean chemical sediments by trace element signatures*. Earth and Planetary Science Letters, 222, 43-60.

Du, J.H., **Zou, C.N.**, **Xu, C.C.**, **He, H.Q.**, **Shen, P.**, **Yang, Y.M.**, **Li, Y.L.**, **Wei, G.Q.**, **Wang, Z.C. & Yang, Y.** 2014. *Theoretical and technical innovations in strategic discovery of a giant gas field in Cambrian Longwangmiao Formation of central Sichuan paleo-uplift, Sichuan Basin*. Petroleum Exploration and Development (abstract in English), 41, 268-277.

Fallon, S.J., White, J.C. & Mcculloch, M.T. 2002. *Porites corals as recorders of mining and environmental impacts: Misima Island, Papua New Guinea*. Geochimica et Cosmochimica Acta, 66, 45-62.

Friedman, I. & O'Neil, J.R. 1977. *Compilation of stale isotope fractionation factors of geochemical interest, in Fleischer, M., ED., data of geochemistry: United States*. Geological Survey Professional Paper 440-KK, 12 p.

Gu, Z.X., He, Y.B., Peng, Y.M., Luo, J.X., Liu, X.F., Zhang, J. & Nie, H.Y. 2019. *"Multiple-lagoon" sedimentary model of the lower Cambrian gypsum-salt rocks in the Sichuan Basin*. Acta Sedimentologica Sinica (abstract in English), 37, 834-846.

Jiang, L., Cai, C., Worden, R.H., Crowley, S.F., Jia, L., Zhang, K. & Duncan, I.J. 2016. *Multiphase dolomitization of deeply buried Cambrian petroleum reservoirs, Tarim Basin, north-west China*. Sedimentology, 63, 2130-2157.

Johannesson, K.H., Hawkins, D.L. & Cortes, A. 2006. *Do Archean chemical sediments record ancient seawater rate earth element patterns?* Geochimica et Cosmochimica Acta, 70, 871-890.

Kaczmarek, S.E. & Sibley, D.F. 2011. *On the evolution of dolomite stoichiometry and cation order during high-temperature synthesis experiments: an alternative model for the geochemical evolution of natural dolomites*. Sediment Geology, 240, 30-40.

Land, L.S. 1980. *The isotopic and trace element geochemistry of dolomite: the state of the art*. In: Zenger D H, Dunham J B, Ethington R L(eds). Concepts and Models of Dolomitization. SEPM Special Publications, 28, 87-110.

Li, X.Z., Guo, Z.H., Wan, Y.J., Liu, X.H., Zhang, M.L., Xie, W.R., Su, Y.H., Hu, Y. & Feng, J.W., 2017. *Geological characteristics and development strategies for Cambrian Longwangmiao Formation gas reservoir in Anyue gas field, Sichuan Basin, SW China*. Petroleum Exploration and Development (abstract in English), 44, 398-406.

Lin, L.B., Hao, Q. & Yu, Y. 2014, *Development characteristics and sealing effectiveness of Lower Cambrian gypsum rock in Sichuan Basin*. Acta Petrologica Sinica (abstract in English), 30, 718-726.

Ma, Z.X., Zhang, W.P., Liu, W. & Li, B. 2012, *Sedimentary characteristics of tidal storm deposit of early Cambrian Qingxudong Formation in the Zhenyuan Area, eastern Guizhou and its palaeogeographical implications*. Acta Sedimentologica Sinica (abstract in English), 30, 787-794.

Machel, H.G. 1997. *Recrystallization versus neomorphism and the concept of 'significant recrystallization' in dolomite research*. Sediment Geology, 113, 161-168.

Machel, H.G. & Anderson, J.H. 1989. P*ervasive subsurface dolomitization of the Nisku Formation in central Alberta*. Journal of Sedimentary Petrology, 59, 891-911.

McKenzie, J.A. 1981. *Holocene dolomitization of calcium carbonate sediments from the coastal sabkhas of Abu Dhabi, U.A.E.: A stable isotope study*. Journal of Geology, 89, 185-198.

Melanie, J.L. 2006. *Isotopes in Palaeoenvironmental Research*. Springer, Netherlands, 231-249 p.

Men, Y.P., Xu, X.S., Mou, C.L., Yu, Q., Yan, J.F. & Liu, W. 2010. *Sedimentary facies and palaeogeography of the evaporates in the middle upper Yangtze area*. Sedimentary Geology and Tethyan Geology (abstract in English), 30, 58-64.

Montańze, I.P., Osleger, D.A., Mack, L.E. & Musgrove, M. 2000. *Evolution of the Sr and C isotope composition of Cambrian oceans*. GSA Today, 10, 1-7.

Mriheel, L.Y. & Anketell, J.M. 2010. *Dolomitization of the early Eocene Jirani dolomite Formation, Gabes-Tripoli Basin, Western of shore, Libya*. Journal of Petrology Geology, 23, 449-474.

Ren, Y., Zhong, D.K., Gao, C.L., Sun, H.T., Meng, H., Hu, X.L., Jiang, Z.C., & Wang, A. 2015. *Characteristics and controlling factors of the lower Cambrian Longwangmiao Formation reservoirs in eastern Sichuan Basin and its adjacent areas*. Journal of Palaeogeography (abstract in English), 17, 829-840.

Ren, Y., Zhong, D.K., Gao, C.L., Yang, X.Q., Xie, R., Li, Z.P., Deng, M.X., & Zhou, Y.C. 2016. *Geochemical characteristics, genesis and hydrocarbon significance of dolomite in the Cambrian Longwangmiao Formation, eastern Sichuan Basin*. Acta Petrolei Sinica (abstract in

English), 37, 1102-1115.

Ren, Y., Zhong, D.K., Gao, C.L., Sun, H.T., Peng, H., Zheng, X.W. & Qiu, C. 2019a. *Origin of dolomite of the lower Cambrian Longwangmiao Formation, eastern Sichuan Basin, China*. Carbonates and Evaporites, 34, 471-490.

Ren, Y., Zhong, D.K., Gao, C.L., Li, B., Cao, X., Wang, A., Dong, Y. & Yan, T. 2019b. *The paleoenvironmental evolution of the Cambrian Longwangmiao Formation (Stage 4, Toyonian) on the Yangtze Platform, South China: petrographic and geochemical constrains*. Marine and Petroleum Geology, 100, 391-411.

Sibley, D.F. & Gregg, J.M. 1987. *Classification of dolomite rock texture*. Journal Sedimentary of Petrology, 57, 967-975.

Sun, H.T., Sun, Y.Y., Liu, H.L., Xie, R, Yang, X.Q. & Ren, Y. 2018. *Typological analysis and genetic mechanism of dolomite in the lower Cambrian Longwangmiao Formation, eastern Sichuan Basin*. Oil & Gas Geology (abstract in English), 39, 318-329.

Vasconcelos, C., McKenzie, J.A., Warthmann, R. & Bernasconi, S. 2005. *Calibration of the $\delta^{18}O$ paleo-thermometer with dolomite formed in microbial cultures and natural environments*. Geology, 33, 317-320.

Veizer, J., Ala, D., Azmy K., Bruckschen, P., Buhl, D., Bruhn, F., Carden, G.A.F., Diener, A., Ebneth S., Godderis, Y., Jasper, T., Korte, C., Pawellek, F., Podlaha, O.G. & Strauss, H. 1999. *$^{87}Sr/^{86}Sr$, $\delta^{13}C$ and $\delta^{18}O$ evolution of Phanerozoic seawater*. Chemical Geology, 161, 59-88.

Wang, P., Liu, X.J. & Sima, L.Q. 2019a. *Grading evaluation and prediction of fracture-cavity reservoirs in Cambrian Longwangmiao Formation of Moxi area, Sichuan Basin, SW China*. Petroleum Exploration and Development (abstract in English), 46, 290-301.

Wang, Y.P., Yang, X.F., Wang, X.Z., Huang, X.S., Chen, C., Yang, Y.M. & Luo, W.J. 2019b. *Reservoir property and genesis of powder crystal dolomite in the Longwangmiao Formation, Moxi Area in central Sichuan Basin*. Geological Science and Technology Information (abstract in English), 38, 197-205.

Yang, X.F., Wang, X.Z., Yang, Y.M., Li, Y.M., Jiang, N., Xie, J.R. & Luo, W.J. 2015. *Diagenesis of the dolomite reservoir in lower Cambrian Longwangmiao Formation in central Sichuan Basin*. Geological Science and Technology Information (abstract in English), 34, 35-41.

Zhang, W.J., Li, S.L., Ren, X.L., Zhang, J., Guo, Y.B., Ye, C.Y. & Chen, Y.N. 2019. *Sedimentary facies characteristics and favorable facies belt distribution of Cambrian Longwangmiao Formation, eastern Sichuan Basin*. Natural Gas Exploration and Development (abstract in English), 42, 56-65.

Zhang, J., Shou, J.F., Zhang, T.F., Pan, L.Y. & Zhou, J.G. 2014. *New approach on the study of dolomite origin: the crystal structure analysis of dolomite*. Acta Sedimentologica Sinica (abstract in English), 32, 550-559.

Zheng, B.G., Mou, C.L., Liang, W., Chen, C., Xu, P.H. & Sun, X.Y. 2016. *Discovery and significance of the storm deposit within the lower Cambrian Qingxudong Formation in the Dingtai Area, northwestern Guizhou*. Acta Geologica Sinica (abstract in English), 34, 478-486.

Zheng, B.G., Mou, C.L., Liang, W. & Chen, C. 2018. *The characteristics of storm deposits of the lower Cambrian Qingxudong Formation in the southeastern margin of Yangtze Platform and its significance*. Acta Geologica Sinica (abstract in English), 92, 1524-1540.

Zhao, H.W. & Jones, B. 2012. *Origin of "island dolostones": a case study from the Cayman Formation (Miocene), Cayman Brac, British West Indies*. Sedimentary Geology, 243-244, 191-206.

Zhao, Y.Y., Zheng, Y.F. & Chen, F.K. 2009. *Trace element and strontium isotope constraints on sedimentary environment of Ediacaran carbonates in southern Anhui, South China*. Chemical Geology, 265, 345-362.

Zhou, J.G., Xu, C.C., Yao, G.S., Yang, G., Zhang, J.Y., Hao, Y., Wang, F., Pan, L.Y., Guo, M.F. & Li, W.Z. 2015. *Genesis and evolution of lower Cambrian Longwangmiao Formation reservoirs, Sichuan Basin, SW China*. Petroleum Exploration and Development (abstract in English), 42, 158-166.

Zhu, C.Q., Hu, S.B., Qiu, N.S., Rao, S. & Yuan, Y.S. 2016. *Thermal history of the Sichuan Basin, SW China: evidence from deep boreholes*. Science China, Earth Sciences (abstract in English), 59, 70-82.

Zou, C.N., Du, J.H., Xu, C.C., Wang, Z.C., Zhang, B.M. Wei, G.Q., Wang, T.S., Yao, G.S., Deng, S.W., Liu, J.J., Zhou, H., Xu, A.N., Yang, Z., Jiang, H. & Gu, Z.D. 2014. *Formation, distribution, resource potential and discovery of the Sinia-Cambrian giant gas field, Sichuan Basin, SW China*. Petroleum Exploration and Development (abstract in English), 41, 278-293.

Received at: 28. 05. 2021
Revised at: 30. 08. 2021
Accepted for publication at: 15. 09. 2021

Published online at: 09. 10. 2021